Influence Relevance Voting: An Accurate And Interpretable Virtual High Throughput Screening Method

S. Joshua Swamidass,*,† Chloé-Agathe Azencott,† Ting-Wan Lin,‡ Hugo Gramajo,§
Shiou-Chuan Tsai,‡ and Pierre Baldi*,†

School of Information and Computer Sciences, Institute for Genomics and Bioinformatics, University of
California, Irvine, Irvine, California 92697-3435, School of Biological Sciences, University of California,
Irvine, Irvine, California 92697-1450, and Microbiology Division, Instituto de Biología Molecular y Celular
de Rosario (IBR), Universidad Nacional de Rosario, Suipacha 531, Rosario, Argentina

Given activity training data from high-throughput screening (HTS) experiments, virtual high-throughput screening (vHTS) methods aim to predict in silico the activity of untested chemicals. We present a novel method, the Influence Relevance Voter (IRV), specifically tailored for the vHTS task. The IRV is a low-parameter neural network which refines a *k*-nearest neighbor classifier by nonlinearly combining the influences of a chemical's neighbors in the training set. Influences are decomposed, also nonlinearly, into a relevance component and a vote component. The IRV is benchmarked using the data and rules of two large, open, competitions, and its performance compared to the performance of other participating methods, as well as of an in-house support vector machine (SVM) method. On these benchmark data sets, IRV achieves state-of-the-art results, comparable to the SVM in one case, and significantly better than the SVM in the other, retrieving three times as many actives in the top 1% of its prediction-sorted list. The IRV presents several other important advantages over SVMs and other methods: (1) the output predictions have a probabilistic semantic; (2) the underlying inferences are interpretable; (3) the training time is very short, on the order of minutes even for very large data sets; (4) the risk of overfitting is minimal, due to the small number of free parameters; and (5) additional information can easily be incorporated into the IRV architecture. Combined with its performance, these qualities make the IRV particularly well suited for vHTS.

Virtual high-throughput screening (vHTS) is the cost-effective, in silico complement of experimental HTS. A vHTS algorithm uses data from HTS experiments to predict the activity of new sets of compounds in silico. Although vHTS is sometimes cast as a classification task, it is more appropriately described as a ranking task, where the goal is to rank additional compounds, such that active compounds are close to the top of the prediction-sorted list as possible. The experiments required to verify a hit are expensive, so it is critical that true actives be recognized as early as possible. Accurately ordering actives by their degree of activity, however, is not critical. The vHTS task, therefore, differs from the "ranking" task of the machine learning literature, in that the goal is not to precisely order the chemicals in relation to each other, but rather to globally rank as many actives as possible above the bulk of the inactives. Furthermore, the data required by methods designed for the machine learning "ranking" task, the complete ranking of active compounds with respect to one another, is often unavailable.

An important algorithm proposed for vHTS is the *k*-nearest neighbor (kNN) classifier, a nonparametric method which has been shown effective in a number of other problems.[1,2] In the kNN approach, each new data point is classified by integrating information from its neighborhood in the training set in a very simple way. Specifically, a new data point is assigned to the class occurring most frequently among its *k* closest structural neighbors in the training set.

While the kNN algorithm has been applied to chemical data, it does not perform optimally[3−6] because all the nearest neighbors contribute equally, regardless of their relative similarities to the test chemical. Hence, important concepts—such as "the more similar a chemical is to its active neighbors, the more likely it is to be active itself" or "the closest neighbors should influence the prediction more than the furthest ones"—are not representable with a kNN. Furthermore, the kNN is usually used to classify, rather than to rank, unknown data. The kNN output can be modified to be an integer between 0 and *k* by counting the number of neighbors that are active, instead of taking a binary majority vote, but even with this quantization, many compounds are mapped to the same integer value and therefore cannot be properly ranked. This is a critical deficiency for vHTS where economic or other reasons may dictate that only a few of the top hits be testable. kNN, even in its quantized version, does not provide a clear ranking of its top hits.

A number of researchers have attempted to rectify these deficiencies of kNN by employing alternate weighing schemes and decision rules.[7−15] In many domains, including vHTS,[9,10] these modifications can substantially improve classification performance. With few exceptions,[10,12,13] however, these modifications are either somewhat ad hoc,

* Corresponding authors. E-mail: sswamida@ics.uci.edu (S.J.S.); pfbaldi@ics.uci.edu (P.B.).
† Institute for Genomics and Bioinformatics, UCI.
‡ School of Biological Sciences, UCI.
§ Universidad Nacional de Rosario.

untuned to the nuances of each data set, or do not produce probabilistic predictions.

Here we propose a novel vHTS method, the Influence Relevance Voter (IRV), which can also be viewed as an extension of the kNN algorithm. The IRV uses a neural network architecture[16-18] to learn how to best integrate information from the nearest structural neighbors contained in the training set. The IRV tunes itself to each data set by a simple gradient descent learning procedure and produces continuous outputs that can be interpreted probabilistically and used to rank all the compounds. We assess the performance of IRV on two benchmark data sets from two recent open datamining competitions. For comparison purposes, we also implement two other methods: MAX-SIM and support vector machines (SVM). MAX-SIM is a particularly simple algorithm, a useful baseline for comparison. In contrast, SVMs are a highly sophisticated class of methods which have been successfully applied to other chemical classification problems[19,20] and are expected to yield high performance on vHTS data sets. Comparisons against the kNN method are not included because the kNN does not rank its hits and, in prior studies, has been consistently outperformed by SVMs on chemical data.

DATA

IJCNN-07 Competition and HIV Data. In 2007, the International Joint Conference on Neural Networks (IJCNN-07)[21] organized the Agnostic Learning versus Prior Knowledge Challenge (ALvPK), a blind prediction competition on five data sets from different fields. One of the data sets used in the competition, the HIV data set, is a vHTS data set. The data set was derived from the Drug Therapeutics Program (DTP) AIDS Antiviral Screen made available by the National Cancer Institute (NCI)[22] The HIV data set contains assay results for 42 678 chemicals experimentally tested for their ability to inhibit the replication of the human immunodeficiency virus in vitro.

The conference organizers processed the raw DTP data in three steps. First, the HIV data was randomly partitioned into a training set consisting of 10% of the chemicals and a testing set composed of the remaining 90%, each labeled with their activity in the screen. Second, the "active" and "moderately active" compounds were combined into a single active class. This processing step, therefore, reduces the number of classes to two. Finally, for each chemical in the HIV data set, the organizers of the competition provided both precomputed feature vectors and the raw chemical structures from which they were extracted. We discard the organizers' feature vectors, preferring to extract our own features.

We constructed cross validation data sets by combining both the training and testing data sets from the competition. Active compounds were defined according to the competitions rules. The details of the data partitions for both the cross validation and competition data sets are summarized in Table 1.

McMaster Competition and DHFR Data. In 2005, the McMaster University organized a vHTS competition using experimental data generated in their laboratories. They screened 99 995 chemicals for inhibition activity against dihydrofolate reductase (DHFR). Inhibitors of DHFR are known to be effective cancer drugs, so both data sets have direct medical relevance. The 99 995 chemicals used in the screen were partitioned into a training and a testing sets of 49 995 and 50 000 chemicals, respectively, all of which are available on the web.[23] For each molecule, two or three assays were performed and the results were reported as the percentage of full DHFR activity achieved in the presence of the test chemical. Lower percentages correspond to higher inhibition. Chemicals were then classified as inhibitors, i.e. active compounds, when all the experimental percentages were below 75%. According to this criterion, less than 0.2% of the data was found to be active.

It is important to note some peculiarities of the protocol used in the McMaster competition. First, the DHFR data contains 315 pairs of duplicate chemicals. These duplicates correspond to identical chemicals tested in solution with, and without, salt ions. Thus, from an experimental standpoint, these duplicate correspond to different experiments. The organizers, however, did not report which salt ions were used in each screen. Additionally, all molecules participating in duplicate tests, irrespective of the salt ions, were classified as inactive. Hence, from a computational standpoint, these duplicates are effectively redundant and should have been removed from the data to accurately assess performance. Second, rather than randomly partitioning the data, the competition organizers decided to increase the task's difficulty by minimizing structural similarity between the chemicals in the training and testing data.[24] At the conclusion of the competition, this decision was criticized by the participants for artificially lowering the performance of similarity-based vHTS methods.

The submissions to this competition are evaluated in the works of Lang et al.[25] and Parker.[26] For comparison purposes, we first conduct tests using the same exact protocol as the one used in the competition, keeping duplicates in the data and using the same training/validation data split. For the cross-validation experiments, however, where the competition rules do not need to be strictly followed, we remove duplicate chemicals from the data. Table 1 details the characteristics of the final data set used in this study.

METHODS

As in most chemoinformatics applications, such as the search of large databases of small molecules[27-29] or the prediction of their physical, chemical, and biological properties,[9,10,19,20,27] all the vHTS methods we implement depend on a quantitative notion of chemical similarity to

Table 1. Number of Positive and Negative Examples in the Training and Testing Datasets Used in the IJCNN-07 and McMaster Competitions, Based on the HIV and DHFR Screens, Respectively[a]

	IJCNN-07 (HIV)			McMaster (DHFR)		
	active	inactive	total	active	inactive	total
train	149	4080	4229	66	49929	49995
test	1354	37095	38449	94	49906	50000
full[b]	1503	41175	42678	160	99520[b]	99680[b]

[a] The IJCNN-07 organizers randomly selected 10% of the data for use as a training set. In contrast, the McMaster organizers partitioned the DHFR data into two equal halves and attempted to minimize chemical similarity between each partition. [b] The last row in the table, labeled "full", shows the size of the nonredundant dataset used for the additional cross-validation experiments.

define the local geometry of chemical space. The underlying intuition, explicitly articulated as the similar property principle,[30] is that the more structurally similar two molecules are, the more likely they are to have similar properties. In turn, the notion of similarity is closely related to how molecules are represented. Thus, in order to precisely define our methods, we must first describe the representations and similarity measures used in this study.

Molecular Similarity and Representations. For this study, we define chemical similarity using a fairly standard fingerprint vector representation. Fingerprints are vectors recording the occurrences of particular substructures within molecular graphs. If we denote a labeled molecular graph with a calligraphic letter, $\mathcal{A}$, and a fingerprint by $\vec{A} = (A_i)$, each component A_i stores a 1-bit (or 0-bit) to indicate the presence (or absence) of a particular substructure in $\mathcal{A}$. Alternatively, each component can store the number of times the corresponding substructure appears in the graph. The resulting fingerprints are very sparse and are often compressed using a lossy algorithm.[31,32] For this study, we use the lossless compression algorithm described elsewhere.[33]

Each component of the fingerprint corresponds to a particular labeled substructure. In terms of labeling, we consider two labelings of the molecular graph, element (E) and element-connectivity (EC). In element labeling, each vertex is labeled by the corresponding atomic symbol (e.g., C for carbon, O for oxygen, N for nitrogen). In element-connectivity labeling, each vertex is labeled by the atomic symbol of the corresponding atom together with the number of heavy atoms to which it is bonded (e.g., C3 for a carbon with three heavy atoms attached). In both labeling schemes, the bonds are simply labeled according to their type (single, double, triple, or aromatic). In terms of graphical substructures, we consider both paths[19,20] of depth d up to 2, 5, or 8 bonds or circular substructures[34] of depth d up to 2 or 3 bonds. Thus the fingerprint components index all the labeled paths, or all the labeled trees, up to a certain depth.

Among the many possible ways of defining similarity between fingerprint vectors,[35] we consider two similarity measures, known to work well with chemical data, the Jaccard−Tanimoto and MinMax measures. In the case of binary fingerprints, the Tanimoto similarity measure is defined by

$$S(\mathcal{A}, \mathcal{B}) = S(\vec{A}, \vec{B}) = \frac{A \cap B}{A \cup B} \tag{1}$$

where $A \cap B$ is the number of 1-bits in both $\vec{A}$ AND $\vec{B}$, and $A \cup B$ is the number of 1-bits that appear (nonexclusively) in either $\vec{A}$ OR $\vec{B}$. In the case of count fingerprints, which record the number of times each substructure occurs in a chemical, previous studies have shown that the MinMax similarity is one of the best performing similarities.[20,36] MinMax is defined by

$$S(\mathcal{A}, \mathcal{B}) = S(\vec{A}, \vec{B}) = \frac{\sum_i \min(A_i, B_i)}{\sum_i \max(A_i, B_i)} \tag{2}$$

where the summations extend over all fingerprint components.

Maximum Similarity. One of the simplest methods for vHTS is the maximum similarity (MAX-SIM) algorithm,[37,38]

in which each test molecule is scored by its highest similarity to a known active compound. Molecules with higher scores (most similar to one of the active molecules) have greater likelihood of being active. Formally, if $\{\mathcal{A}_1, ..., \mathcal{A}_{|\mathcal{A}|}\}$ is the set containing all known active compounds and S is a similarity measure between two molecular fingerprints, the output of the predictor, $z(\mathcal{X})$, for the test chemical, $\mathcal{X}$, is given by

$$z(\mathcal{X}) = \max_{\mathcal{A} = \mathcal{A}_1}^{\mathcal{A}_{|\mathcal{A}|}} S(\mathcal{X}, \mathcal{A}) \tag{3}$$

MAX-SIM is trivial to implement, does not require any parameter tuning, has been well studied,[37,38] and is intuitively simple. The resulting predictions yield a ranking and are somewhat interpretable; by examining the active compound the most similar to the query molecule and the corresponding similarity score, one can gain insight into the rationale behind the prediction. This method, however, takes very little information into account since, for instance, it discards all experimental information about inactive compounds. More refined methods, which consider all of the training data, can be expected to perform better.

Support Vector Machines. Alternatively, vHTS can be formulated as a machine learning classification task and solved with an SVM.[4,39] As the MinMax and Tanimoto metrics both satisfy Mercer's condition,[20] we can apply the standard SVM algorithm to score a compound $\mathcal{K}$ according to the prediction function

$$z(\mathcal{X}) = \sum_{\mathcal{T} = \mathcal{T}_1}^{\mathcal{T}_{|\mathcal{T}|}} \alpha_{\mathcal{T}} S(\mathcal{X}, \mathcal{T}) + \alpha_0 \tag{4}$$

where $\mathcal{T}$ ranges over the training set. The $\alpha_{\mathcal{T}}$ weights are associated with each training example and learned from the data using a quadratic programming algorithm which maximizes the separation between active and inactive chemicals with a solution that fixes the majority of the $\alpha_{\mathcal{T}}$s to zero. The nonzero $\alpha_{\mathcal{T}}$s correspond to the support vectors which help define the decision boundary.

Two technical problems, associated with vHTS data sets, arise when attempting to apply a standard SVM implementation. First, vHTS data sets are much larger than typical SVM data sets. Using N as the number of examples in the training data set, the standard formulation of SVM solved by quadratic programming, requires $O(N^2)$ memory usage and $O(N^3)$ processing time, quickly becoming very slow as data sets increase to the size of vHTS experiments. Fortunately, faster SVM algorithms have been developed. We use the SVMTorch online SVM implementation[40] with memory-usage scaling like $O(N)$ and training time scaling like $O(N^2)$.

Second, vHTS data is often extremely unbalanced. The HIV data set, for instance, has about 28 times as many inactive examples as active examples. Unbalanced data sets are not always well learned by SVM algorithms, which generally assume a more balanced class distribution. The most straightforward strategy for dealing with class imbalance is to control the sensitivity, i.e. the C parameter, which limits the magnitude of each $\alpha_{\mathcal{T}}$ of the SVM.[41,42] Misclassified instances of the under-represented class can be more penalized by assigning a higher sensitivity to the under-

ACCURATE AND INTERPRETABLE vHTS METHOD

J. Chem. Inf. Model., Vol. 49, No. 4, 2009 **759**

represented class. In our case, however, this method does not lead to significant improvements.

A more complex strategy, referred to as "oversampled SVMs" in the literature, adjusts for class imbalance by training ensembles of SVMs on class-balanced subsets of the training data.[43,44] In this study, we build balanced subsets of the training data by splitting the inactive data into partitions of about the same size as the active data. Each of these partitions is then combined with the entire data set of active compounds to form a collection of data sets on which to train an ensemble of SVMs. At the final stage, the predicted classes (0 for inactive and 1 for active) of each SVM are summed to produce a final score. The higher this score, the more likely the test molecule is to be active. The resulting ensembles of SVMs are abbreviated as E-SVM. However, when data sets have only a small total number of instances in the under-represented class, E-SVM requires a high number of individual SVMs to be trained on a very small number of data points. For example, the McMaster data set requires 750 individual SVMs to be trained on only 122 data points. SVMs are likely to perform poorly on such small training sets. Therefore, we are only able to apply this method to the HIV data set.

These SVM-based methods yield accurate predictors. These predictors, however, are black-boxes, which are not easy to interpret beyond the information provided by the support vectors. The SVM decision function ignores representative examples, which are typically far from the decision boundary. Consequently, it is difficult to tease out exactly which experimental evidence suggests how a particular test compound should be classified. Furthermore, all the data's modeling power is used to learn the decision boundary; the posterior probability distribution of the data is not directly learned. Consequently, the output of an SVM, especially far away from the decision boundary, does not always correlate well with the confidence of a prediction.[45] This deficiency is problematic in vHTS, where ranking active compounds at the top of the prediction list is more important than learning a single decision boundary between classes.

Influence Relevance Voter. The Influence Relevance Voter (IRV) uses a neural network to combine information from the neighbors of a chemical to estimate its probability of being active. The input to the network is the list of labeled nearest neighbors and their similarities to the chemical, possibly with some variations described below. While many neural network architecture are possible, here we propose a specific implementation which uses the concept of weight-sharing to reduce the number of free parameters, hence avoiding overfitting.[16,17,46] This algorithm addresses deficiencies of the SVM-based algorithms by directly modeling the posterior probability distribution of the data. Furthermore, the IRV naturally exposes the data used to classify each test instance in an interpretable way.

At a high-level, the IRV is defined by a preprocessing step, during which all the neighbors of a test molecule are identified, and a processing step, during which information from each neighbor is fed into a neural network to produce a prediction. The prediction is computed from the "influence" of each neighbor, which in turn is computed as the product of each neighbor's "relevance", encoding how much each neighbor should affect the prediction, and "vote", encoding the direction toward which the prediction should be pushed.
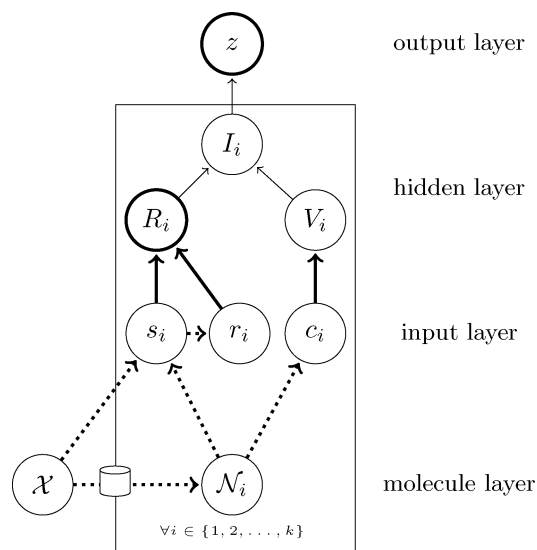

Figure 1. Neural network architecture of the IRV using a notation similar to the plate notation of graphical models. The structure and weights depicted inside the plate are replicated for and shared with each neighbor i. Thick lines depicts elements of the graph learned from the data. Dotted lines depict portions of the network computed during the preprocessing step, during which the test chemical $\mathcal{X}$ is used to retrieve a list of neighbors, $\{\mathcal{N}_1, ..., \mathcal{N}_k\}$ from all the chemicals in the training data. The directed influences I_i of each neighbor are summed up to into a logistic output node to produce the final prediction, $z(\mathcal{X})$.

Figure 1 shows the architecture of the IRV, using a notation similar to the plate notation used for graphical models, which displays the local dependencies that are replicated throughout the network, illustrating its structure and exposing the extensive weight-sharing across the network.

Formally, we compute the IRV's output as,

$$z(\mathcal{X}) = \sigma\left(w_z + \sum_{i=1}^{k} I_i\right) \quad (5)$$

where $\mathcal{X}$ is the test molecule, i ranges from 1 to k over all the k nearest neighbors, I_i is the "influence" of the ith neighbor on the output, w_z is the bias of the output node, and $\sigma(\cdot)$ is the logistic function $1/(1 + e^{-x})$. These influences indicate exactly how much, and in which direction, each training example contributes to the prediction and can be used to interpret each final prediction. The influence of the ith node is defined by

$$I_i = R_i V_i \quad (6)$$

where R_i is the relevance and V_i is the vote of the ith neighbor. For this study, the relevance is defined as

$$R_i = \sigma(w_y + w_s s_i + w_r r_i) \quad (7)$$

where s_i is the similarity $S(\mathcal{X}, \mathcal{N}_i)$ of the ith closest neighbor to the test compound, r_i is the rank of the ith neighbor in the similarity-sorted list of neighbors, w_s and w_r are parameters tuning the importance of different inputs, and w_y is the bias of the logistic unit. In order to facilitate learning, all inputs are normalized into standard units during the preprocessing step, by subtracting the corresponding mean

and dividing by the corresponding standard deviation. For this study, we define the vote by

$$V_i = \begin{cases} w_0 & \text{if } c_i = 0 \\ w_1 & \text{if } c_i = 1 \end{cases} \qquad (8)$$

where w_0 is the weight associated with inactive neighbors, w_1 is the weight associated with active neighbors, and $c_i \in \{0,1\}$ is the class of the ith neighbor.

The logistic output of the IRV can be interpreted as a probability and directly encodes the confidence of each prediction[18,47]

$$z(\mathcal{X}) \approx P(\mathcal{X} \text{ is active}|\mathcal{X}\text{'s structure, training data}) \qquad (9)$$

In other words, the output of the network on a test molecule is approximately equal to the probability of the test molecule being active given its structure and the training data. This is enforced by training the network to minimize the relative-entropy or Kullback−Leibler divergence between the true target distribution $t(\mathcal{T})$ and the predicted distribution $z(\mathcal{T})$ across all molecules $\mathcal{T}$ in the training set.[18] Thus the IRV is trained by gradient descent to minimize the error or, equivalently, the negative log-likelihood given by

$$-\sum_{\mathcal{T}} t(\mathcal{T}) \log z(\mathcal{T}) + (1 - t(\mathcal{T})) \log(1 - z(\mathcal{T})) \qquad (10)$$

It is possible to add weight decay terms to the error function, equivalent to defining a Gaussian prior on the weights, to prevent overfitting during training. In practice, overfitting is unlikely because so few parameters are optimized during training. Three parameters, w_s, w_r, and w_y, are shared across all k neighbors. The model requires just three additional parameters, w_1, w_0, and w_z. Therefore, a total of only six parameters are learnt from the data. Nevertheless, weight decay is included in this implementation because it seems to further decrease the training time. The corresponding penalized negative log-likelihood is given by

$$\sum_w w^2 - \sum_{\mathcal{T}} [t(\mathcal{T}) \log z(\mathcal{T}) + (1 - t(\mathcal{T})) \log(1 - z(\mathcal{T}))] \qquad (11)$$

where the first summation is over all six weights.

Each influence, I_i, encodes how much, and in what direction, its associated neighbor pushes the prediction. Influences with the greatest absolute values affect the output the most, their associated neighbors are the data upon which the prediction is made. Those with negative values push the output toward an inactive prediction, while those with positive values push the output toward an active prediction. Thus the influences and the prediction are readily under-standable by direct inspection and visualization.

Variations on the IRV. The IRV's performance can be fine-tuned by several variations. In this study, we particularly consider: (1) the number of neighbors selected; (2) the class-balance of the neighbors; and (3) the weighing of different classes during training. More complex variations are explored in the discussion.

The network can be presented different total numbers k of neighbors. The network's performance is not sensitive to the exact value of k above a certain threshold, but sometimes

small performance improvements can be realized. For the competitions, we fixed k at 20 and were able to obtain good results with low computational cost.

Rather than presenting the IRV network with nearest neighbors irrespective of their class, it is possible instead to present an equal number of neighbors from each class. For example, instead of selecting the 20 nearest neighbors, one can select both the 10 nearest active and the 10 nearest inactive compounds. The latter is most effective in situations where the number of active compounds is particularly small (e.g., the DHFR data set).

During training, it is also possible to overweigh the log-likelihood of one of the classes, so as to increase its contribution to the training process. This can be used to address the class imbalance in most vHTS data sets. For example, if there are 20 times more inactive chemicals than active ones, then the error associated with each of the active compounds can be multiplied by 20 during training to restore the balance. Initial experiments indicate that this variation does not appreciably improve performance, so this variation is excluded from the results.

In any case, the IRV comes with a relatively small number of hyperparameters, primarily the number k of neighbors and their composition, and inferences regarding their values can be made from the statistical properties of the data, as in the case of other machine learning methods.

Performance Measures. Each of the vHTS algorithms we describe, MAX-SIM, SVM, and IRV, outputs a number for each chemical in the uknown data set. This number is used to rank the data set and it is the ranks of the true actives that are used by different metrics to quantify performance and assess each method.

The IJCNN-07 competition determines winners according to the balanced error rate (BER) metric. This metric requires to set a threshold, learned during the training stage, to separate predicted actives from predicted inactives. Once this is done, the BER is defined as the average of the proportion of actives mistakenly predicted as inactives and the propor-tion of inactives mistakenly predicted as actives. The lower the BER score, the better the method is at separating classes.

Whenever the participants associate a list of prediction values, rather than binary classes, with their submission, the IJCNN-07 competition also reports the area under the ROC curve (AUC). The ROC curve plots the true positive rate (TPR), which is the proportion of correctly predicted actives, against the false positive rate (FPR), which is the proportion of inactives incorrectly predicted as actives, for every possible threshold. The higher the AUC, the better the method is at separating classes.

In the McMaster competition, performance is assessed according to the number of active compounds retrieved in the top 1% and top 5% of the prediction-ranked test data. This is equivalent to looking at the enrichment factor ($EF_{f\%}$), which is the proportion of active compounds retrieved in the first f percent of the ranked list of chemicals.

In addition to these metrics, we also report for each data set the value of the Boltzmann-enhanced discrimination of the receiver operating characteristic (BEDROC) metric with α fixed at 20.0. The BEDROC metric, which quantifies the ability of a method to rank active compounds early at the top of the prediction-sorted test data, is particularly suitable to the evaluation of vHTS methods. Additional details about

ACCURATE AND INTERPRETABLE vHTS METHOD

J. Chem. Inf. Model., Vol. 49, No. 4, 2009 **761**

Table 2. Each Experiment's Optimal Hyperparameters, in Terms of Similarity Scheme (Labeling, Feature Type, and Metric) and Whether or Not the Class-Balance of IRV's Nearest Neighbors is Enforced[a]

	competition rules		cross-validation	
	HIV	DHFR	HIV	DHFR
label	E	EC	EC	EC
feature	trees ($d \leq 2$)	paths ($d \leq 8$)	trees ($d \leq 2$)	paths ($d \leq 8$)
metric	MinMax	Tanimoto	Tanimoto	MinMax
balanced	no (20)	yes (10 + 10)	no (20)	yes (10 + 10)

[a] If class-balance is enforced, the IRV is presented the 10 nearest active neighbors and the 10 nearest inactive neighbors (10 + 10); otherwise, the IRV is presented 20 nearest neighbors (irrespective of class). The optimal hyperparameters are always consistent across all methods and across all folds of the cross-validation experiments.

Table 3. Performance of Several Methods on the HIV Data Used in the IJCNN-07 Competition[a]

	competition rules			cross-validation		
	BEDROC	BER	AUC	BEDROC	BER	AUC
IJCNN-07	NA	0.283	**0.771**	NA	NA	NA
random	0.035	0.500	0.500	0.035	0.500	0.500
IRV	*0.500*	*0.271*	0.762	**0.630** (0.633)	*0.210* (0.208)	**0.845** (0.839)
E-SVM	0.465	**0.269**	*0.764*	0.573	**0.199**	*0.845*
SVM	**0.507**	0.280	0.758	*0.616*	0.217	0.836
MAX-SIM	0.439	0.283	0.739	0.526 (0.515)	0.225 (0.222)	0.806 (0.811)

[a] The IJCNN-07 row shows the best performance submitted to the competition not including results submitted by our laboratory. The random row shows the performance of a random classifier. Leave-one-out cross-validation performances are displayed between parentheses; all other cross-validation performances are 10-fold cross-validations. A value that is not available is denoted by NA. Best performances are in **bold,** and second-best performances are in *italics*.

assessing early recognition and the mathematical derivation of the BEDROC metric can be found in the work of Truchon and Bayly.[48]

RESULTS

We report the cross-validation performance of the MAX-SIM, SVM, and IRV methods on both the HIV and DHFR data sets. In order to directly compare our methods with others, we also present the performance of each method obtained while following the IJCNN-07 and McMaster competition protocols. Table 2 reports the hyperparameters (the similarity scheme and neighbor selection protocol) which yield the best performance for each experiment. The best similarity scheme is consistent across all methods and all folds of the cross-validation within each experiment.

HIV Cross-Validation. The various vHTS methods are evaluated by cross-validation on the HIV data. The performance is computed by averaging 10 random 10-fold cross-validated performances, using for each fold 90% of the data for training and 10% of the data for validation. Detailed results are described in Table 3. When feasible, we also report the leave-one-out (LOO) cross-validation performance. The SVM and E-SVM require about 1000 s to train each fold, which amounts to approximately 500 CPU-days to LOO cross-validate the full data set. Therefore, the SVM LOO performances are excluded.

The IRV achieves the highest BEDROC of 0.630. The best BER of 0.1993, however, is obtained by the E-SVM. Both SVM and E-SVM are clearly behind the IRV in terms of BEDROC performance, with values of 0.616 and 0.530, respectively. The ROC curves for the HIV data are plotted in Figure 3. These curves demonstrate that the SVM and IRV are approximately equivalent for this task and that the E-SVM does not perform as well in the critical early part of the ROC curve.

Figure 2 illustrates how easy it is to intepret the IRV prediction, by tracking and visualizing the underlying influences corresponding to the experimental evidence used in order to make a prediction. Visualizing the IRV influence's is much more informative than explanations derived from an SVM, which prunes most of the experimental data from the final model.

The IJCNN-07 Competition. We participated in the IJCNN-07 competition by entering our E-SVM and IRV predictions for the HIV data set in the Prior Knowledge track. As the competition was judged by BER, the E-SVM won first place with a BER of 0.2693 and the IRV took second place with a BER of 0.2782. The IRV's performance was not fully optimized at the time, and we now report a BER of 0.2705, slightly above the winning entry. Thus again on this dataset, the performance of the IRV is at least equal to the performance of the SVM-based methods. Table 3 reports the performance of the MAX-SIM, SVM, and IRV methods in comparison with both a random classifier and the best participants in the IJCNN-07 experiment.

Although the BER was used to select the winners of the competition, the BEDROC metric better evaluates the suitability of methods for the vHTS problem. The best BEDROC of 0.507 is obtained with the SVM instead of the E-SVM. The IRV still ranks just behind the SVM, with a BEDROC of 0.500.

In the case of the SVM-based methods, there may be a tradeoff between BER and BEDROC performance. For this data set, the E-SVM optimizes the BER, but ranks third in BEDROC performance. The SVM optimizes the BEDROC, but ranks third in BER performance. The IRV, in contrast, is a close second in both BER and BEDROC performance, suggesting that it may optimize both performances simultaneously. Altogether, these results suggest that the IRV method is slightly more suitable for vHTS, but E-SVM can better optimize the global class separation, quantified by the BER in the IJCNN-07 competition.

DHFR Cross-Validation. We also cross-validate our methods on the DHFR data set. Performances are computed by averaging the results of ten random 10-fold cross-validations. We also report the LOO cross-validation performance of both the MAX-SIM and IRV methods.

The performance of our methods on the full, nonredundant data is reported in Table 4. The optimal performances are reached using the relaxed criteria for assigning actives and presenting the IRV with the 10 nearest active neighbors and 10 nearest inactive neighbors. Retrieving 20.6% of the actives in the top 5% of the ranked list, the SVM performs much better than both the random classifier and MAX-SIM, which retrieves only 8.8% of the actives in the same fraction. The IRV performs much better, retrieving 25% of the active compounds in the top 5% of the prediction-sorted data. The superiority of the IRV over the SVM is also apparent in its
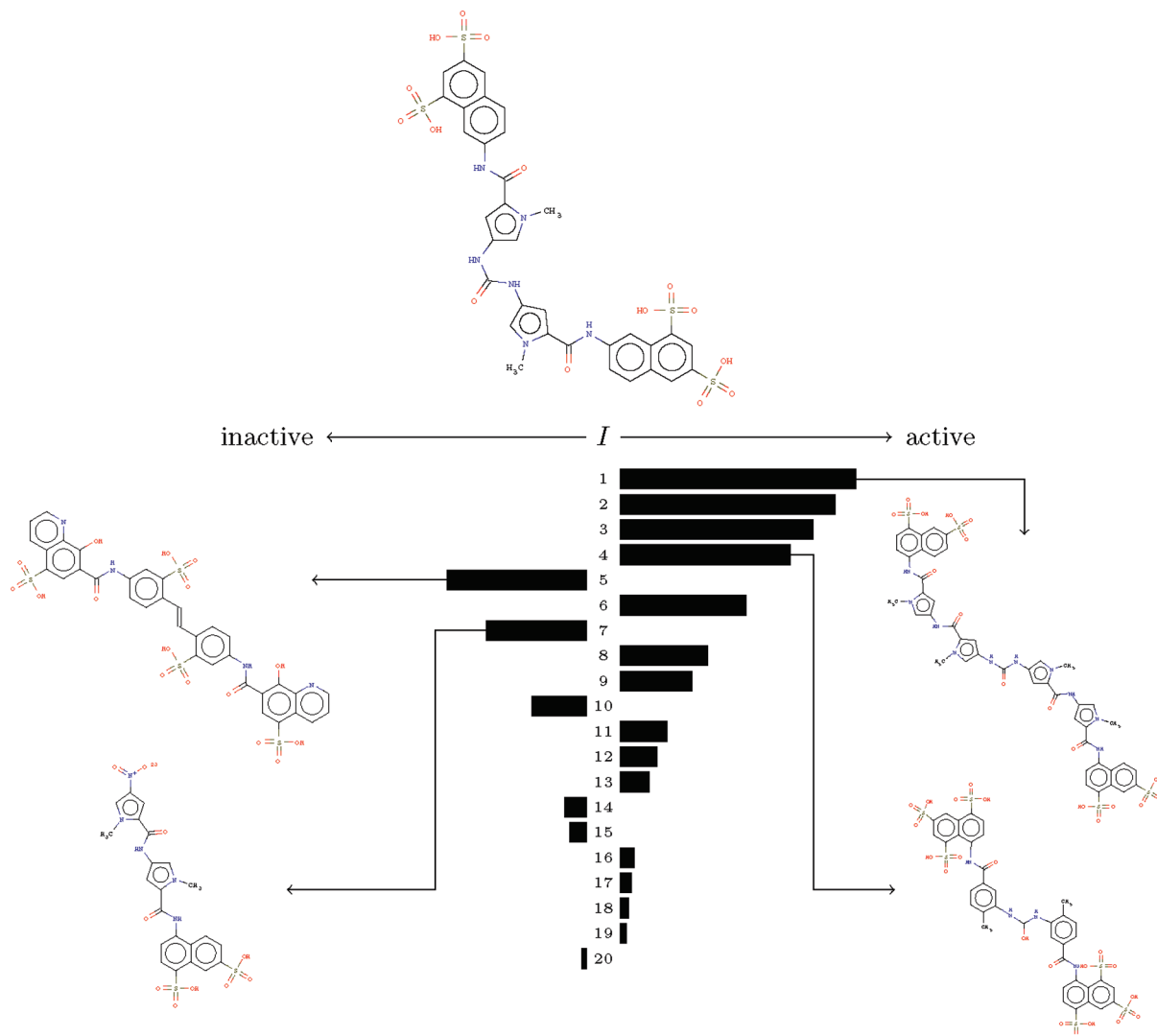
Figure 2. Influences on an accurately predicted hit from the HIV data set, obtained in the cross-validation experiment, displayed as a bar graph. The IRV used to compute these influences was trained using the 20 nearest neighbors. The experimental data both supporting and countering the prediction is readily apparent. The structures of four neighbors, two actives and two inactives, are shown. Compounds on the right are structurally similar and active. Compounds on the left are structurally similar and inactive.

BEDROC performance of 0.251 for the IRV versus 0.200 for the SVM. Furthermore, of the top 20 IRV predictions, nine were true actives. The top twelve hits are listed in Figure 4. The nearly ideal ranking of the top hits was not duplicated by the SVM.

The cross-validated ROC curves for the DHFR data are displayed in Figure 5. Consistently with the performance metrics, these curves clearly show the superiority of the IRV on this particularly challenging data set.

The McMaster Competition. We did not enter any of our predictors in the McMaster competition, which took place before the beginning of this work, but we do retrospectively compare our results, following the competition rules, to published results. The winners were picked based on the number of actives ranked in the top 1% and 5% of the predictions. This is equivalent to looking at the enrichment factors (EF) calculated at 1% and 5%. For this competition, even the winner was only able to correctly retrieve a small fraction of the active chemicals in the test set: 2 in the top 1% and 13 in the top 5% of the prediction-ranked output. A detailed comparison of the performances obtained while following the competition rules are presented in Table 4.

For the IRV, optimal results are achieved by presenting the 10 nearest active neighbors and 10 nearest inactive neighbors to the network. Furthermore, for all the classifiers, optimal results are obtained using the relaxed criterion to label actives during training. For the relaxed criterion, instead of labeling active compounds when both experimental scores are less than 75%, we label compounds active if at least one score is below 75%. This increases the pool of positive examples during training, feeding the classifiers additional information. Actives are assigned by the relaxed criterion *only* during training; test performance are computed using the more stringent competition criterion to ensure our results are comparable with the literature.

Both the SVM and the MAX-SIM method perform worse than random, retrieving only 4.2% and 3.1% of the actives respectively, in the top 5% of their prediction-ranked lists. This performance is similar to most submissions to the competition, as 29 out of 32 participants also retrieved 4.2% of hits in the top 5% of their ranked list, and only one of them also found more than 1.1% of hits in the top 1%.

The IRV, in contrast, detects almost 14% (13 out of 94) of the actives in the top 5% of the ranked list, which is as
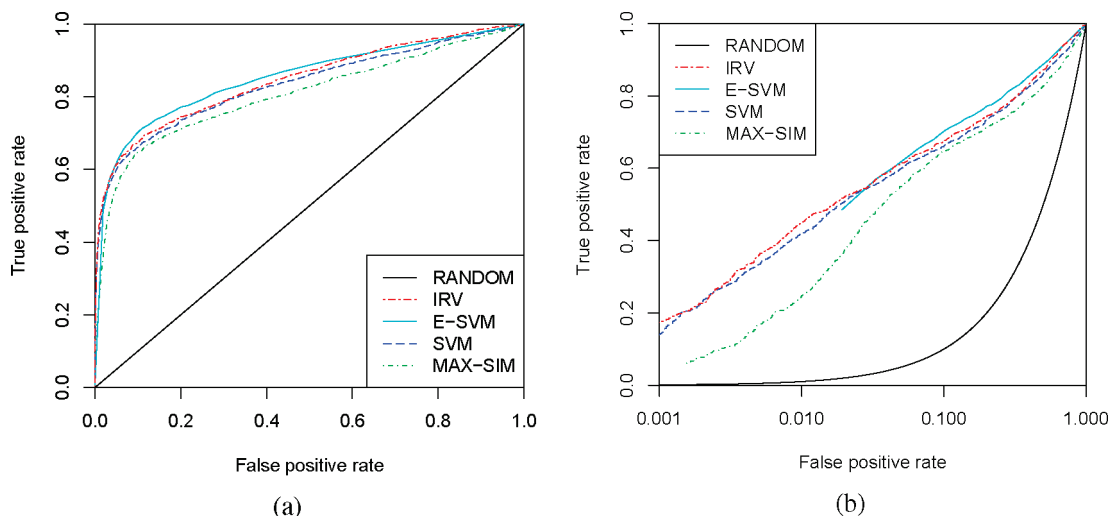
ACCURATE AND INTERPRETABLE vHTS METHOD

J. Chem. Inf. Model., Vol. 49, No. 4, 2009 **763**

Figure 3. 10-fold cross-validated performances of various algorithms on the full HIV data displayed using (1) a standard ROC curve and (2) a pROC curve. The pROC curve plots the false positive rate on a logarithmic axis to emphasize the crucial initial portion of the ROC curve.[49]

Table 4. Results from the DHFR Dataset Used in the McMaster competition[a]

	competition rules			cross-validation		
	BEDROC	1%	5%	BEDROC	1%	5%
McMaster	NA	2	**13**	NA	NA	NA
random	0.002	0.9	4.7	0.002	1.6	8.0
IRV	**0.100**	**3**	**13**	**0.251** (0.258)	*20* (23)	**40** (44)
SVM	*0.084*	1	4	*0.200*	**22**	*33*
MAX-SIM	0.045	0	3	0.062 (0.069)	4 (4)	13 (14)

[a] The random row shows the performance of a random classifier. Leave-one-out cross-validation performances are displayed between parentheses; all other cross-validation performances are 10-fold cross-validations. A value that is not available is denoted by NA. Best performances are in **bold**, and second-best performance are in *italics*.

good as the best entry in the competition. Moreover, the IRV detects one more active in the top 1% of the prediction-sorted data than this best entry. Altogether, these results show that the IRV performs much better than the SVM and slightly better than the best methods in the community on this challenging data set.

Although the results from the McMaster competition provide a useful basis for performance comparison, the organizers did not maintain any information regarding the exact methods used by each participant. As a result, information regarding the methods used to generate the competition's best entry, for instance, is not readily available.

DISCUSSION

According to metrics best suited to evaluate vHTS, the IRV compares favorably with SVMs and other state-of-the-art methods. On the HIV data set, the IRV performance is comparable to the best SVM performance, while on the DHFR data set the IRV performance is clearly superior to SVMs. In addition to outperforming SVMs, the IRV is preferable because (1) it is trained much more quickly; (2) it provides a framework which easily allows the incorporation of additional information, beyond the chemical structures; and (3) its predictions are interpretable.

IRV Training Time. A first advantage of the IRV is that it is quickly trained, once the nearest neighbors have been computed. Each chemical is represented using only a small number of informative features, allowing the neural network to be trained in minutes rather than hours or days, and making leave-one-out cross-validation possible, even on very large data sets. Learning the weights is efficient, with both space and time complexity scaling approximately as $O(N \cdot k)$. This corresponds to the fact that, under typical conditions, neural network training converges in a constant number of epochs (one epoch corresponding to one training pass through the training set). Thus the IRV training complexity scales like the complexity of computing its full gradient.

Finding the nearest neighbors requires much more time than learning the weights. Although computing the neighbors is computationally expensive, it is trivially parallelizable and less expensive than training an SVM. The naive algorithm, using a full pairwise comparison of the training data, requires $O(N^2 \log k)$ time. The pruning search algorithms described in the work of Swamidass and Baldi[29] can reduce the complexity to approximately $O(N^{1.6} \log k)$. Furthermore, finding the nearest neighbors is trivially distributed across an arbitrary number C of computers, with negligible overhead. The complexity of the parallelized algorithm for finding neighbors, therefore, can be approximated as $O(N^{1.6}/C \log k)$.

Alternatively, locality-sensitive hashing (LSH) could be used to find most of the nearest neighbors in only $O(N \log N)$ time, enabling predictions in $O(\log N)$ time, further reducing the complexity.[50] LSH, however, is an approximate algorithm and is not guaranteed to find all the neighbors exactly. In principle, the IRV may be able to tolerate the noise introduced by inexact nearest-neighbor algorithms, but this possibility is beyond the scope of this study and currently untested.

Although the weights can be trained quickly by gradient descent, the IRV requires the manual selection of a few hyperparameters, such as the number of nearest neighbors and the way they are pooled and ordered. The IRV, however, does not appear to be highly sensitive to these parameters. Selecting the 20 nearest neighbors seems to be about right for the two data sets studied. There still remains some reason to believe information may be hidden among distant neighbors, especially when one class is particularly rare.[8] In principle, both the information from distant neighbors can be included and the
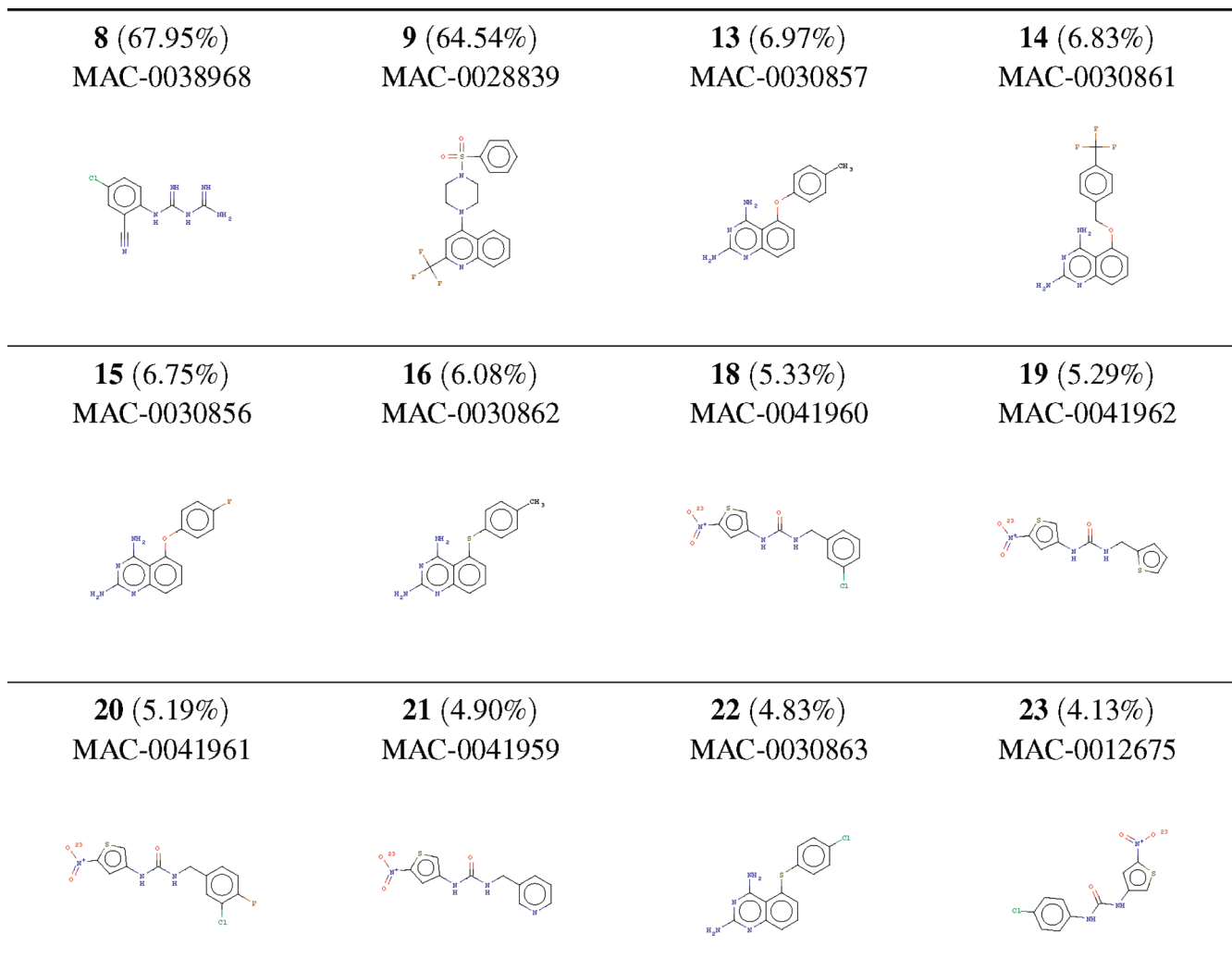
8 (67.95%)
MAC-0038968

9 (64.54%)
MAC-0028839

13 (6.97%)
MAC-0030857

14 (6.83%)
MAC-0030861

15 (6.75%)
MAC-0030856

16 (6.08%)
MAC-0030862

18 (5.33%)
MAC-0041960

19 (5.29%)
MAC-0041962

20 (5.19%)
MAC-0041961

21 (4.90%)
MAC-0041959

22 (4.83%)
MAC-0030863

23 (4.13%)
MAC-0012675

Figure 4. Top twelve accurately predicted hits by an IRV cross-validated on the McMaster data set. Prediction-sorted rankings are in **bold**, and the IRV outputs are in parentheses. Strikingly, the top hits are ranked at the very top of the prediction-sorted list. Although they exhibit a high degree of similarity, the top hits have several different scaffolds.
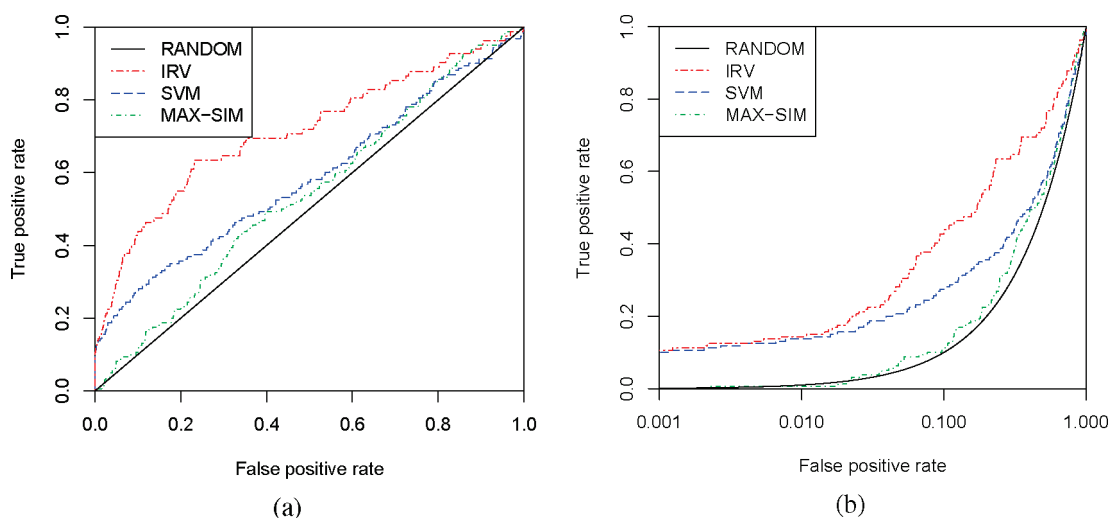
Figure 5. 10-fold cross-validated performances on the DHFR data. (a) ROC; (b) pROC curve. The pROC curve plots the FPR on a logarithmic axis to emphasize the crucial first portion of the ROC curve.[49]

arbitrariness inherent in picking k can be removed by setting $k = \infty$ and presenting the network with *all* instances in the training set instead of just the nearest few neighbors. Unfortunately, this does increase the time and space complexity of training and

classification. This variation is also beyond the scope of this study and left for future work.

IRV Incorporation of Additional Information. A second advantage of the IRV is that it can naturally be extended to
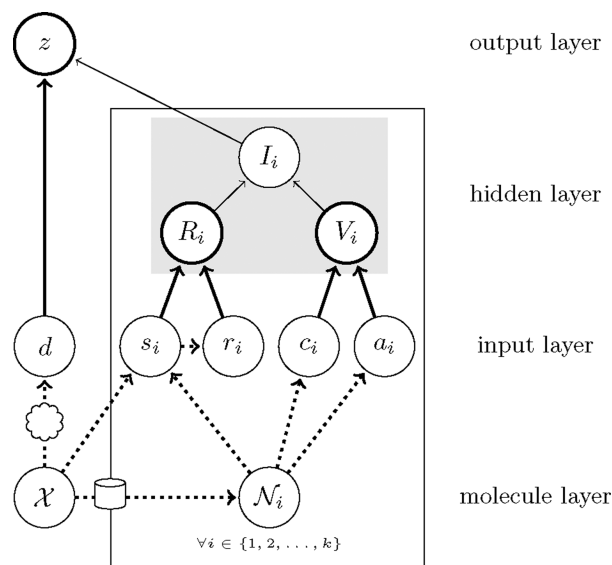
Figure 6. Examples of IRV architectural extensions. The variable d denotes the docking score derived by fitting each test chemical, $\mathcal{X}$, into the binding pocket of a known protein target, depicted as a cloud in the figure. The grayed out rectangle delimits a portion of the network which could be trivially replaced with an arbitrarily complex neural network to generate an IRV with increased modeling power; additional replaceable portions can be imagined. The variable a_i denotes the real-valued activity of each neighbor, $\mathcal{N}_i$, in the HTS screen.

cohesively integrate additional types of information. Several of these extensions are visually depicted in Figure 6. In the case of the HIV data set, compounds classified as active for IJCNN-07 are in fact known to be either "active" or "moderately active", the distinction between which is ignored. We can, however, learn the predictive value of the chemicals belonging to the "moderately active" class by adding another class of neighbors to the IRV model. This amounts to redefining V_i as

$$V_i = \begin{cases} w_0 & \text{if} \quad c_i = 0 \\ w_1 & \text{if} \quad c_i = 1 \\ w_2 & \text{if} \quad c_i = 2 \end{cases} \tag{12}$$

where, for the neighbors, w_0, w_1, and w_2, corresponding to inactive, moderately active, or active compounds. Of course, if the aim is to find active compounds as defined by the competition, the likelihood function used during training would remain unchanged, with the "moderately active" compounds labeled as active compounds. The IRV can be modified in similar ways to use the raw inhibition data, a_i, reported in the DHFR data set, by using

$$V_i = w_a a_i + w_v \tag{13}$$

where w_a and w_v are learned from the data. More generally, one could define

$$V_i = f(a_i, c_i) \tag{14}$$

where $f(\cdot)$ is a parametrized function—with parameters to be learned from the data—of both the inhibition data and the assigned class of each neighbor. Initial experiments indicate that these modifications can further optimize performance.

Instance-level data, also, can easily be integrated in the IRV framework. For example, solubility is known to be an important property that can affect the ability of an HTS experiment to measure the activity of a compound. Feeding the test compound's predicted solubility into the output node could improve prediction accuracy. Likewise, in situations where the structure of the target protein is available, such as for the McMasters competition, performance gains could be realized by feeding the docking energy of the test compound directly into the output node, naturally integrating docking and similarity data into the same predictor.

Similarly, it is possible to replace portions of the IRV with neural networks of arbitrary complexity, thereby increasing the modeling power. This comes of course at a cost of increasing the number of parameters which must be learned, requiring the model to be trained on increasing amounts of data.

IRV Interpretability. A third advantage of the IRV is that its predictions are transparent. The exact experimental data used to make a prediction can be extracted from the network by examining each prediction's influences. Thus, although the IRV is composed of a neural network, it should be considered a "white-box" method. In contrast, the predictions of an SVM are more difficult to interpret. Along the same lines, the IRV's output is probabilistic and directly encodes each prediction's uncertainty, enabling reasonably accurate estimation of the number of hits in an arbitrary set of test molecules. Although an SVM output can be rescaled onto a probability scale,[51−53] SVMs can exhibit a tendency to predict with overly high confidence in regions where the training data is sparse.

Often, there is a tradeoff between understandable models and high performing models,[1,54] requiring researchers to choose if interpretability is more important than accuracy. The IRV seems to solve this dilemma by yielding high performance on HTS data using an easily understandable framework.

REFERENCES AND NOTES

(1) Karakoc, E.; Cherkasov, A.; Sahinalp, S. C. Distance Based Algorithms For Small Biomolecule Classification And Structural Similarity Search. *Bioinformatics* **2006**, *22*, 243.

(2) Zheng, W.; Tropsha, A. Novel Variable Selection Quantitative Structure-Property Relationship Approach Based on the k-Nearest-Neighbor Principle. *J. Chem. Inf. Comput. Sci.* **2000**, *40*, 185–194.

(3) Cannon, E. O.; Bender, A.; Palmer, D. S.; Mitchell, J. B. O. Chemoinformatics-Based Classification of Prohibited Substances Employed for Doping in Sport. *J. Chem. Inf. Model.* **2006**, *46*, 2369–2380.

(4) Geppert, H.; Horvath, T.; Gartner, T.; Wrobel, S.; Bajorath, J. Support-Vector-Machine-Based Ranking Significantly Improves the Effectiveness of Similarity Searching Using 2D Fingerprints and Multiple Reference Compounds. *J. Chem. Inf. Model.* **2008**, *48*, 742–746.

(5) Plewczynski, D.; Spieser, S. A. H.; Koch, U. Assessing Different Classification Methods for Virtual Screening. *J. Chem. Inf. Model.* **2006**, *46*, 1098–1106.

(6) Simmons, K.; Kinney, J.; Owens, A.; Kleier, D.; Bloch, K.; Argentar, D.; Walsh, A.; Vaidyanathan, G. Comparative Study of Machine-Learning and Chemometric Tools for Analysis of In-Vivo High-Throughput Screening Data. *J. Chem. Inf. Model.* **2008**, *48*, 1663–1668.

(7) Hastie, T.; Tibshirani, R. Discriminant Adaptive Nearest Neighbor Classification and Regression. *Adv. Neural. Inform. Process. Syst.* **1996**, 409–415.

(8) Holmes, C.; Adams, N. Likelihood inference in nearest-neighbour classification models. *Biometrika* **2003**, *90* (14), 99–112.

(9) Kozak, K.; Kozak, M.; Stapor, K. Weighted k-Nearest-Neighbor Techniques for High Throughput Screening Data. *Int. J. Biomed. Sci* **2006**, *01*, 155–160.

(10) Niwa, T. Using General Regression and Probabilistic Neural Networks To Predict Human Intestinal Absorption with Topological Descriptors Derived from Two-Dimensional Chemical Structures. *J. Chem. Inf. Comput. Sci.* **2003**, *43*, 113–119.

(11) Shang, W.; Qu, Y.; Zhu, H.; Huang, H.; Lin, Y.; Dong, H. An Adaptive Fuzzy kNN Text Classifier Based on Gini Index Weight. *ISCC '06: Proceedings of the 11th IEEE Symposium on Computers and Communications*, Pula-Cagliari, Sardinia, Italy, June 26–29, 2006; pp 448−453.

(12) Specht, D. Probabilistic neural networks for classification, mapping, or associative memory. *IEEE International Conference on Neural Networks*, San Diego, California, July 24–27, 1988; Vol. 1, pp 525−532.

(13) Specht, D. A general regression neural network. *IEEE Trans. Neural Networks* **1991**, *2*, 568–576.

(14) Tan, S. Neighbor-weighted K-nearest neighbor for unbalanced text corpus. *Expert Syst. Appl.* **2005**, *28*, 667–671.

(15) Zhang, H.; Berg, A. C.; Maire, M.; Malik, J. SVM-KNN: Discriminative Nearest Neighbor Classification for Visual Category Recognition. *Proceedings of CVPR 2006*, New York, New York, June 17–22, 2006; Vol. 2, pp 2126−2136.

(16) Bishop, C. In *Neural Networks for Pattern Recognition*; Oxford University Press, Inc: New York, 1995; Chapter 1.

(17) Baldi, P. Gradient descent learning algorithm overview: a general dynamical systems perspective. *IEEE Trans. Neural Networks* **1995**, *6*, 182–195.

(18) Baldi, P.; Brunak, S. *Bioinformatics: the machine learning approach*, 2nd ed.; MIT Press: Cambridge, MA, 2001.

(19) Azencott, C. A.; Ksikes, A.; Swamidass, S. J.; Chen, J. H.; Ralaivola, L.; Baldi, P. One- to Four-Dimensional Kernels for Virtual Screening and the Prediction of Physical, Chemical, and Biological Properties. *J. Chem. Inf. Model.* **2007**, *47*, 965–974.

(20) Swamidass, S. J.; Chen, J. H.; Bruand, J.; Phung, P.; Ralaivola, L.; Baldi, P. Kernels for Small Molecules and the Prediction of Mutagenicity, Toxicity, and Anti-Cancer Activity. *Bioinformatics* **2005**, *21*, 359.

(21) Agnostic Learning vs. Prior Knowledge Challenge. http://www.agnostic.inf.ethz.ch/index.php (accessed Jan 15, 2009).

(22) DTP - AIDS Antiviral Screen Data. http://dtp.nci.nih.gov/docs/aids/aids_data.html (accessed Jan 15, 2009).

(23) HTS Data Mining and Docking Competition. http://hts.mcmaster.ca/HTSDataMiningandDockingCompetition.html (accessed Jan 15, 2009).

(24) Bender, A.; Mussa, H. Y.; Glen, R. C. Screening for Dihydrofolate Reductase Inhibitors Using MOLPRINT 2D, a Fast Fragment-Based Method Employing the Naïve Bayesian Classifier: Limitations of the Descriptor and the Importance of Balanced Chemistry in Training and Test Sets. *J. Biomol. Screen* **2005**, *10*, 658–666.

(25) Lang, P. T.; Kuntz, I. D.; Maggiora, G. M.; Bajorath, J. Evaluating the high-throughput screening computations. *J. Biomol. Screen.* **2005**, *10*, 649–652.

(26) Parker, C. N. McMaster University data-mining and docking competition: computational models on the catwalk. *J. Biomol. Screen.* **2005**, *10*, 647–648.

(27) Leach, A. R.; Gillet, V. J. *An Introduction to Chemoinformatics*; Springer: Dordrecht, The Netherlands, 2005.

(28) Chen, J.; Swamidass, S. J.; Dou, Y.; Bruand, J.; Baldi, P. ChemDB: A Public Database Of Small Molecules And Related Chemoinformatics Resources. *Bioinformatics* **2005**, *21*, 4133–4139.

(29) Swamidass, S. J.; Baldi, P. Bounds and Algorithms for Exact Searches of Chemical Fingerprints in Linear and Sub-Linear Time. *J. Chem. Inf. Model.* **2007**, *47*, 302–317.

(30) *Concepts and Applications of Molecular Similarity*; Johnson, M. A., Maggiora, G. M., Eds.; John Wiley: New York, 1990.

(31) Flower, D. R. On the Properties of Bit String-Based Measures of Chemical Similarity. *J. Chem. Inf. Comput. Sci.* **1998**, *38*, 378–386.

(32) Raymond, J. W.; Willett, P. Effectiveness of Graph-Based and Fingerprint-Based Similarity Measures for Virtual Screening of 2D Chemical Structure Databases. *J. Comput. Aided Mol. Des.* **2001**, *16*, 59–71.

(33) Baldi, P.; Benz, R.; Hirschberg, D.; Swamidass, S. Lossless compression of chemical fingerprints using integer entropy codes improves storage and retrieval. *J. Chem. Inf. Model.* **2007**, *47*, 2098–2109.

(34) Hassan, M.; Brown, R. D.; Varma-O'Brien, S.; Rogers, D. Cheminformatics analysis and learning in a data pipelining environment. *Mol. Divers.* **2006**, *10*, 283–299.

(35) Holliday, J. D.; Hu, C. Y.; Willett, P. Grouping of coefficients for the calculation of inter-molecular similarity and dissimilarity using 2D fragment bit-strings. *Comb. Chem. High Throughput Screen.* **2002**, *5*, 155–66.

(36) Ralaivola, L.; Swamidass, S. J.; Saigo, H.; Baldi, P. Graph Kernels for Chemical Informatics. *Neural Networks* **2005**, *18*, 1093–1110.

(37) Hert, J.; Willett, P.; Wilton, D. J.; Acklin, P.; Azzaoui, K.; Jacoby, E.; Schuffenhauer, A. Comparison of Fingerprint-Based Methods for Virtual Screening Using Multiple Bioactive Reference Structures. *J. Chem. Inf. Model.* **2004**, *44*, 1177–1185.

(38) Hert, J.; Willett, P.; Wilton, D. J.; Acklin, P.; Azzaoui, K.; Jacoby, E.; Schuffenhauer, A. Enhancing the effectiveness of similarity-based virtual screening using nearest-neighbor information. *J. Med. Chem.* **2005**, *48*, 7049–54.

(39) Mahé, P.; Ralaivola, L.; Stoven, V.; Vert, J. P. The Pharmacophore Kernel for Virtual Screening with Support Vector Machines. *J. Chem. Inf. Model.* **2006**, *46*, 2003–2014.

(40) Collobert, R.; Bengio, S. SVMTorch: Support Vector Machines for Large-Scale Regression Problems. *J. Mach. Learn. Res* **2001**, *1*, 143–160; http://www.idiap.ch/learning/SVMTorch.html.

(41) Veropoulos, K.; Campbell, C.; Cristianini, N. Controlling the Sensitivity of Support Vector Machines. *Proceedings of the International Joint Conference on AI*, Stockholm, Sweden, July 31−August 6, 1999; pp 55−60.

(42) Shin, H.; Cho, S. How to Deal with Large Dataset, Class Imbalance and Binary Output in SVM based Response Model. *Proceedings of the Korean Data Mining Conference*, Seoul, Korea, 2003; pp 93−107.

(43) Estabrooks, A.; Jo, T.; Japkowicz, N. A Multiple Resampling Method for Learning From Imbalanced Data Set. *Comput. Intell.* **2004**, *20*, 18–36.

(44) Orriols, A.; Bernad-Mansilla, E. The Class Imbalance Problem in Learning Classifier Systems: A Preliminary Study. *Proceedings of the 2005 Workshops on Genetic and Evolutionary Computation*, Washington, D.C., June 25−26, 2005; pp 74−78.

(45) Tipping, M. E. Sparse Bayesian Learning and the Relevance Vector Machine. *J. Mach. Learn. Res.* **2001**, *1*, 211–244.

(46) Baldi, P.; Pollastri, G. The principled design of large-scale recursive neural network architectures DAG-RNNS and the protein structure prediction problem. *J. Mach. Learn. Res.* **2003**, *4*, 575–602.

(47) Dybowski, R.; Roberts, S. J. Confidence intervals and prediction intervals for feed-forward neural networks. *Clin. Appl. Artif. Neural Networks* **2001**, 298–326.

(48) Truchon, J. F.; Bayly, C. I. Evaluating Virtual Screening Methods: Good and Bad Metrics for the "Early Recognition" Problem. *J. Chem. Inf. Model.* **2007**, *47*, 488–508.

(49) Clark, R. D.; Webster-Clark, D. J. Managing Bias in ROC Curves. *J. Comput.-Aided Mol. Des.* **2008**, *22*, 141–146.

(50) Dutta, D.; Guha, R.; Jurs, P.; Chen, T. Scalable partitioning and exploration of chemical spaces using geometric hashing. *J. Chem. Inf. Model.* **2006**, *46*, 321–333.

(51) *Probabilities for Support Vector Machines*; Smola, A. J., Bartlett, P., Scholkopf, B., Schuurmans, D., Eds.; MIT Press: Cambridge, MA, 1999; pp 61−74.

(52) Sollich, P. Probabilistic interpretations and Bayesian methods for support vector machines. Artificial Neural Networks, *ICANN 99. Ninth International Conference on Neural Networks*, Edinburgh, U.K., September 7–10, 1999; Vol. 1, pp 91−96, pub. no. 470.

(53) Kwok, J. T. Y. Moderating the outputs of support vector machine classifiers. *IEEE Trans. Neural Networks* **1999**, *10*, 1018–1031.

(54) Szafron, D.; Lu, P.; Greiner, R.; Wishart, D. S.; Poulin, B.; Eisner, R.; Lu, Z.; Anvik, J.; Macdonell, C.; Fyshe, A.; Meeuwis, D. Proteome Analyst: Custom Predictions with Explanations in a Web-based Tool for High-throughput Proteome Annotations. *Nucleic Acids Res.* **2004**, *32*, 365.